Arab J. Nucl. Sci. Appl., Vol. 52, 2, 169-180 (2019)

Arab Journal of Nuclear Sciences and Applications

ISSN 1110-0451 ***Web site: ajnsa.journals.ekb.eg*** **(ESNSA)**

Estimation of the Most Appropriate Threshold for Lesion Delineation and Volumetric Quantification in ^{18}F-FDG PET

Shaban Alramlawy[1], Abdel Gawad H [2], Magdy Khalil[3] and Medhat W. Shafaa[3]

[1] *Department of Critical Care, Faculty of Medicine, - Cairo University Hospitals Cairo University, Cairo, Egypt*

[2]*Faculty of Medicine, Nuclear Medicine and Oncology center, Cairo University Hospitals Cairo University, Egypt*

[3] *Department of Physics (Medical Biophysics), Faculty of Science, Helwan University, Helwan, Egypt*

Received 7th May 2018
Accepted 17th Mar.2019

The function formulation to estimate the most appropriate percentage value of maximum Standardized uptake value as a threshold for automatic lesion delineation in PET/CT exam considering lesion to background ratio and the lesion volume determined by computed tomography "CT" tissue segmentation software was investigated. The phantom consists of two parts: a hollow cylinder of a diameter (18.6 cm), length (21.6 cm), and multiple spheres. The sphere assembly contains 4 spheres of different volumes. The phantom was filled with water containing 18F-Fluorodeoxyglucose (18F-FDG) forming the sphere versus background activity concentration (µCi/ml) ratios 3:1, 5:1, 8:1, 10:1, 12:1, 14:1 and15:1. For each scan, the sphere set is aligned in the center of the field of view "FOV" and the time per bed position is similar to that of the routine work 3min. Graphs were plotted of standardized uptake value threshold versus lesion-size at different sphere/background ratio using MS Excel. There was a logarithmic decrease in threshold with an increase in lesion size. The most appropriate SUV threshold for each lesion at different lesion/background was estimated from the plotted graphs. Four tests namely, (5:1, 8:1, 12:1 and 15:1) were used to generate a 3D general function to estimate threshold using the contrast ratio and lesion volume as inputs and the other three tests (3:1, 10:1 and 14:1) were used for the function validation. The Normalized mean square error (NMSE) is used to measure the convergence between estimated and measured data set. The created logarithmic functions offer an easy and simple way to estimate the percentage value of SUV max as a threshold using the lesion/background ratio and sphere volume(or Diameter) from CT images as inputs to be used for lesion delineation and volume determination in PET images that were verified and the NMSE=6.2. It could be concluded that the created formula is useful and easy to estimate the most appropriate SUV threshold for automatically definite lesion volume.

Keywords: Positron emission tomography-computed tomography, SUV, Lesion delineation

Introduction

F18-FDG is glucose analog and it is the most widely used radiopharmaceutical in positron emission tomography (PET). F18-FDG uptake in the tissue cells reflects the activity of this tissue. Cancer cells need more glucose than normal cells, and this is obviously demonstrated in the PET scanning [1]. The location and activity of any lesion can be determined and this helps in case management. The lesion location determination is supported when combining computed tomography with PET in one scanner. PET/CT allows determination of metabolic tumor volume (MTV) and consequently total lesion glycolysis (TLG) [2]. TLG has a significant predictive value in oncology since it reflects the change in status and response to treatment [3], [4]. Also for appropriate detection of gross tumor volume (GTV), the PET images are used in radiotherapy planning [5]. The metabolism inhomogeneity in some tumor shown by PET

Corresponding author: Hesham_ag@yahoo.com
DOI: 10.21608/ajnsa.2019.3449.1080

images directs the oncologist to give the accurate dose to the patient according to the lesion activity [6].Currently, the tumor is delineated either by observation or guided by CT which is variable according to personal experience [7]-[8]. The relatively low spatial resolution of PET and noise contribution results in ill-defined lesion boundaries. Many studies on automatic lesion delineation using percentage value of maximum standardized uptake value (SUV max) were conducted in an attempt to obtain an optimum threshold for appropriate lesion delineation and the most commonly used thresholds are 40% or 50% of SUV max within the volume of interest [2], [9]. Other automatic PET delineation methods include contrast-oriented [10], gradient-based [11], adaptive thresholding [9], background-subtracted relative-threshold level [12] and statistical modeling (FLAB) [13] and their performance have been compared in several studies [15]-[16]. In the present study, standard hollow spheres with well-known volume were used to accurately determine the optimum percentage of SUVmax as a threshold for lesions delineation considering the contrast ratio.

Materials and Methods

Phantom study

The phantom images were acquired using a dedicated PET-CT scanner Ingenuity TF 64 (Philips Healthcare, Cleveland, OH, USA). This scanner combines a modular, LYSO-based PET component with a 64-channel CT component. The phantom consists of two parts: a hollow cylinder of a diameter (18.6 cm) and length (21.6 cm), and multiple spheres. The sphere assembly contains six spheres of varying volume ranging from 0.5 mL to 16 mL (i.e., 0.5,1, 2, 4, 8 and 16 mL) and internal diameters ranging from 9.9mm to 31.2mm (i.e. 9.9, 12.4, 15.6, 19.7,24.8 and 31.2 mm) .The spheres with volume 0.5 mL (9.9mm diameter) and 1 mL (12.4mm diameter) are excluded from this study.

Phantom preparation and scanning

The phantom was filled with a mixture of water and 18F-FDG to make the sphere versus background activity concentration (μCi/ml) ratios as 3:1, 5:1, 8:1, 10:1, 12:1, 14:1 and 15:1. In each experience and at each time, the spheres are placed accurately in the center of FOV. The Phantom was scanned with the routinely used protocol and the time/ bed position set to be 3 min.

Data analysis

The Sphere volumes were delineated automatically using various thresholds as, 30 %, 40%, 50%, 60%, 70% and 80% (percentage of maximum SUV). This was carried out for every lesion volume in the different seven concentration experiments as mentioned above.

Graphs of the threshold versus lesion-volume for each sphere/background ratio using MS Excel function are plotted as in Figures (2, 4). The functions represent the relationship between the threshold values and the lesion sizes are listed in Tables as in (1, 2, 3, 4, 6, 7 and 8).

Computed tomography image segmentation

As the medical imaging technology has seen a tremendous growth, there are a number of methods available as well as images generated daily in health care. The difference in these images due to different parts of the body through various methods have been satisfactorily analyzed in different need to develop a sophisticated and effective image makes the development of sophisticated and effective image segmentation techniques. In the study, the lesion volume was calculated using the image segmentation tools impeded in the manufacturer processing program as shown in Fig. (1).

Function formulation

For each lesion volume in contrast ratios 5:1, 8:1, 12:1 and 15:1, the sphere SUV max and the background SUV mean were measured, then the ratio was calculated (lesion/ background).

The curve of each sphere indicates best threshold through which a result of lesion size closer to the known one was calculated. The different lesion volumes on different contrast ratios, the measured ratios, and the thresholds were then listed in Table (5). Then MS-Excel was used to draw a relationship between contrast ratio, sphere volume and threshold as shown in Fig. (3). The data form showed clearly that the relationship is logarithmic and then a commercially available Excel adds-ins called ThredDify was used to generate a 3D form to estimate the lesion threshold considering the contrast ratio and lesion volume as inputs in Eq.(18):

$$z = 87.7 + \ln(x^{-14.3} \times y^{-5.9}) \qquad \text{Eq.18}$$

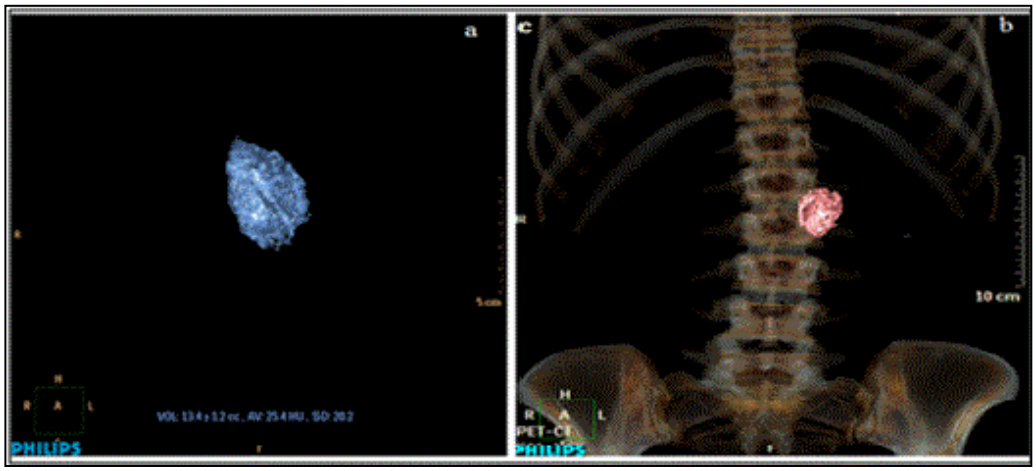

Fig. (1): (a) the segmented lesion and its volume, (b) the 3D rendering and the anatomical lesion site

Function validation

For the other three tests, 3:1, 10:1 and 14:1, the appropriate threshold and the contrast ratios were measured in the same way as previously mentioned in other experiments. In addition, the measured contrast ratios and the well-known lesion volumes were used to get the estimated threshold using Eq. (18). The measured and calculated thresholds, are listed in Table (9). Normalized Mean Square Error (NMSE) (Eq.1) used to

A group of routine cases was randomly selected. For each lesion, a region of interest (ROI) in CT in the 2D image was used to calculate the lesion Hounsfield Unit (HU). This value was used as a threshold in the tissue segmentation tool to extract the lesion from the rested part of the body and then calculate the lesion volume.

For the same lesion, the Lesion/Background was calculated, using the PET images, by measuring the SUV max for the lesion and the mean SUV (SUV mean) for the background. This value (lesion/background) was used in addition to the lesion volume to calculate the most appropriate threshold by substitution in the formulated function. When using this threshold for lesion delineation, as a result, the lesion volume in PET can be obtained and then compared to that from the tissue segmentation of CT images to verify the result**.**

Results

Function generation

Figure (2) displays the relation between the threshold and sphere volume at contrast ratio 5:1, measure and validate the convergence between the measured and data generated from the proposed equation.

$$NMSE = 100 \times \sqrt{\frac{\sum_1^n (x_m - x_e)2}{n}} \qquad (1)$$

Where x_m is the measured data and x_e is the estimated data

Clinical applications

8:1, 12:1 and 15:1 and the trend line equations are listed in Tables (1-4).

The most appropriate threshold for every lesion volume is calculated from its relative trend line equation and tabulated in Table (5)

A logarithmic data fit using Three Dify Excel add-ins was performed which resulted in the formulation of the following equation

$$\boldsymbol{z = 87.7 + \ln(x^{-14.3} \times y^{-5.9})} \qquad \text{Eq.18}$$

Where x is the contrast ratio, y is the sphere volume and z is the percentage of maximum SUV

Knowing that, Sphere volume $= \frac{4}{3}\pi r^3$, Diameter (D) =2r The Eq.18 Can be reformulated as follows using Diameter instead of volume:

$$\boldsymbol{z = 91.3 - 14.3\ln(x) - 17.7\ln(D)} \qquad \text{Eq.19}$$

Where x is the contrast ratio and D is the sphere Diameter

Function validation

For function validation concentration ratios 3:1, 10:1 and 14:1 were used as in the same way for function formation and the relative graphs are illustrated in Fig. (4)

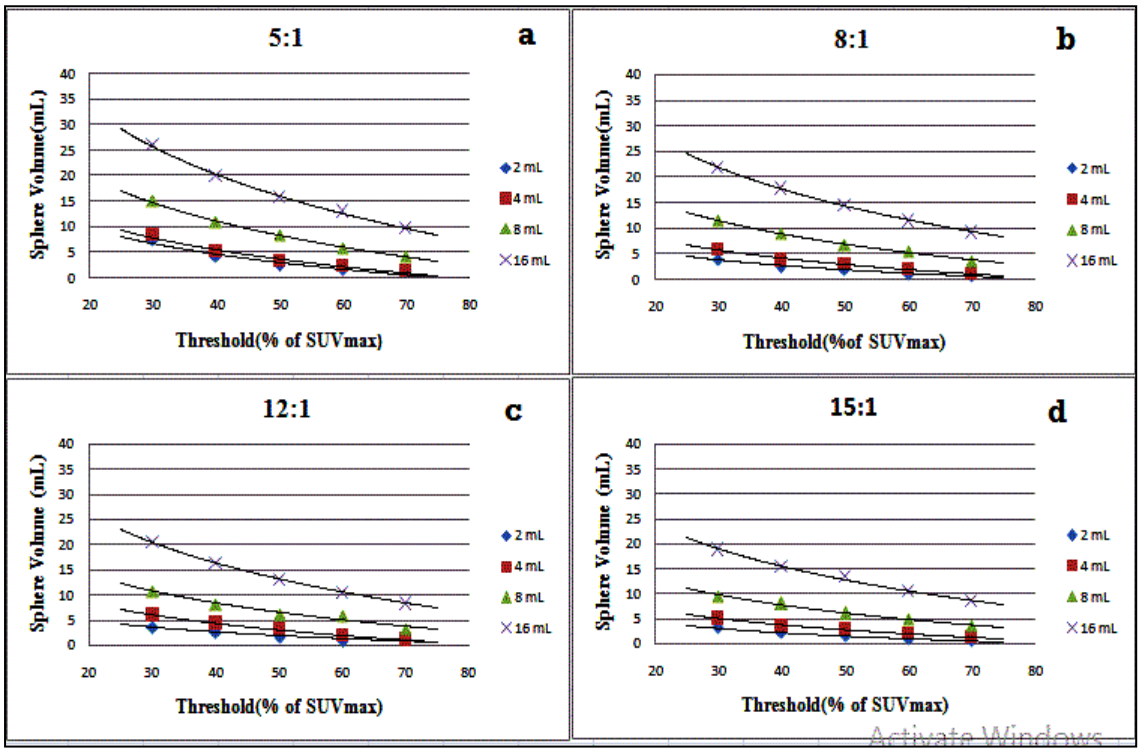

Fig. (2): The relation between threshold and sphere volume at contrast ratio (a) contrast ratio 5:1, (b) 8:1 ,(c) 12:1 and (d) 15:1 used for function formation

TABLE (1): SET OF FUNCTIONS RELATING THRESHOLD AND SPHERE VOLUME AT CONTRAST RATIO 5 TO 1

Sphere Volume(mL)	Contrast ratio 5:1	R^2	Equation No.
2	$y = -3.44ln(x) + 15.79$	0.98	(2)
4	$y = -4.7\ln(x) + 22.5$	0.99	(3)
8	$y = -12.2ln(x) + 56.42$	0.99	(4)
16	$y = -19.1ln(x) + 90.98$	0.99	(5)

TABLE (2): SET OF FUNCTIONS RELATING THRESHOLD AND SPHERE VOLUME AT CONTRAST RATIO 8 TO 1

Sphere Volume(mL)	Contrast ratio 8:1	R^2	Equation No.
2	$y = -3.42\ln(x) + 15.03$	0.98	(6)
4	$y = -5.18\ln(x) + 23.42$	0.98	(7)
8	$y = -9.23\ln(x) + 43.03$	0.99	(8)
16	$y = -15.4\ln(x) + 74.06$	0.99	(9)

TABLE (1): SET OF FUNCTIONS RELATING THRESHOLD AND SPHERE VOLUME AT CONTRAST RATIO 12 TO 1

Sphere Volume(mL)	Contrast ratio 12:1	R^2	Equation No.
2	$y = -4.11\ln(x) + 17.6$	0.98	(10)
4	$y = -5.74\ln(x) + 25.49$	0.97	(11)
8	$y = -8.89\ln(x) + 40.9$	0.99	(12)
16	$y = -14.3\ln(x) + 69$	0.99	(13)

TABLE (2): SET OF FUNCTIONS RELATING THRESHOLD AND SPHERE VOLUME AT CONTRAST RATIO 15 TO 1

Sphere Volume(mL)	15:1	R^2	Equation No.
2	$y = -2.74\ln(x) + 12.36$	0.98	(14)
4	$y = -4.31\ln(x) + 19.9$	0.99	(15)
8	$y = -7.37\ln(x) + 34.99$	0.99	(16)
16	$y = -12.60\ln(x) + 62.02$	0.99	(17)

Table (3): Most appropriate threshold values at different contrast ratios and sphere volumes

Contrast Ratio		**Volume(cm^3)**	**Lesion/Background**	**Best threshold (% of SUVmax)**
Lesion /Background	**5:1**	**2**	**3.395**	**54**
		4	**3.913**	**52**
		8	**4.098**	**51.5**
		16	**4.506**	**51**
	8:1	**2**	**6.296**	**45**
		4	**6.814**	**44**
		8	**6.889**	**44**
		16	**6.778**	**43**
	12:1	**2**	**10.574**	**43**
		4	**10.669**	**42**
		8	**10.909**	**40**
		16	**11.148**	**39**
	15:1	**2**	**11.607**	**41.5**
		4	**13.25**	**40**
		8	**13.178**	**39**
		16	**13.321**	**38**

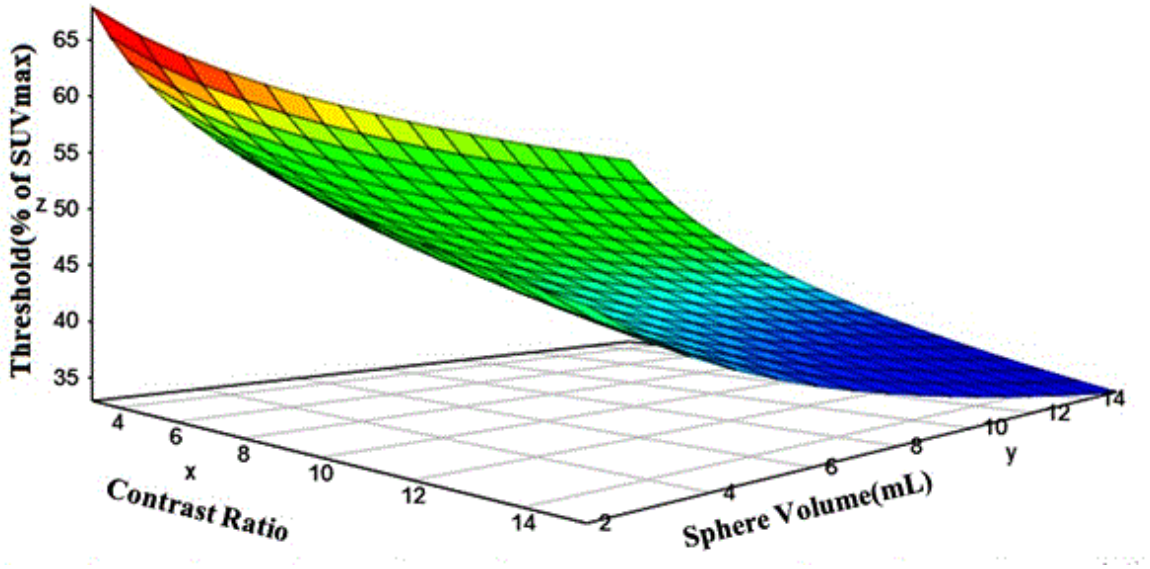

Fig. (3): Relation between contrast ratio, lesion volume and threshold

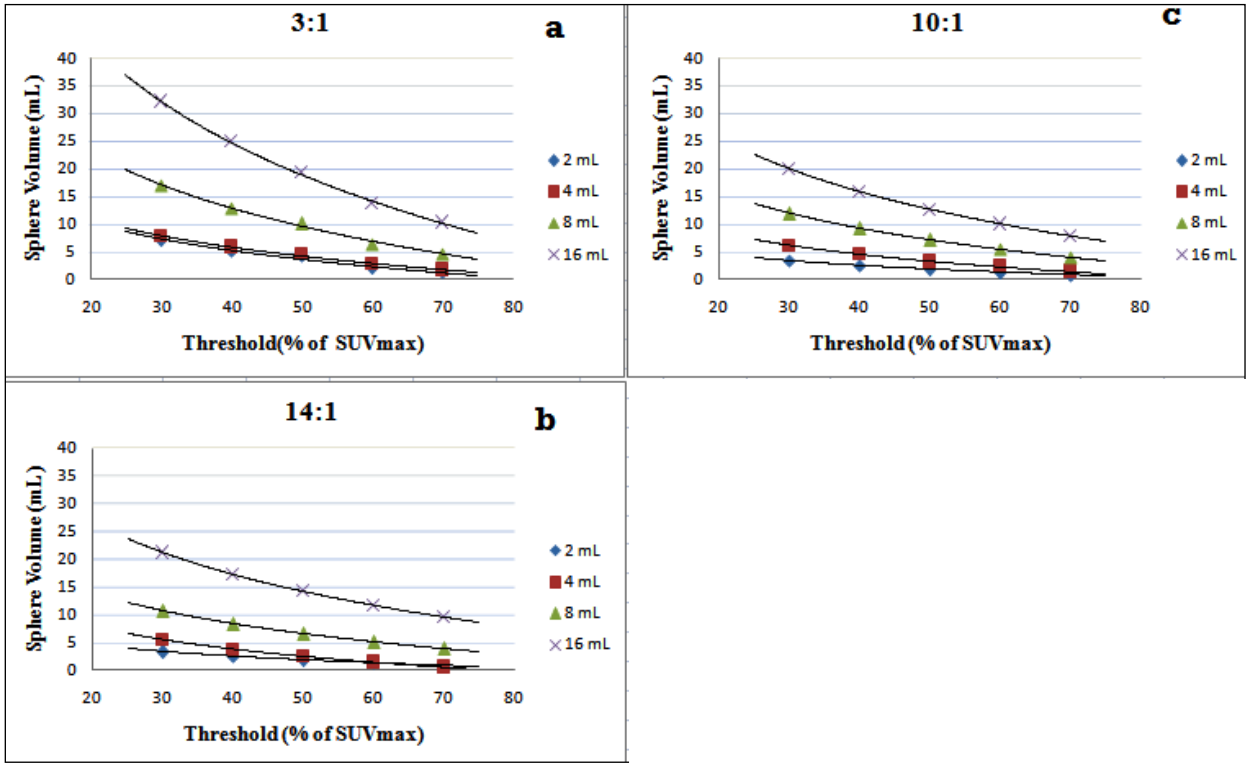

Figure (4) the relation between threshold and sphere volume at contrast ratio (a) 3:1, (b) 10:1 and (c) 14:1 used for function validation

TABLE (4): SET OF FUNCTIONS RELATING THRESHOLD AND SPHERE VOLUME AT CONTRAST RATIO 3 TO 1

Sphere Volume(mL)	3:1	R^2	Equation No.
2	y = -6.58ln(x) + 29.55	0.92	(20)
4	y = -7.01ln(x) + 31.75	0.97	(21)
8	y = -14.3ln(x) + 65.69	0.98	(22)
16	y = -25.6ln(x) + 119.4	0.99	(23)

TABLE (5): SET OF FUNCTIONS RELATING THRESHOLD AND SPHERE VOLUME AT CONTRAST RATIO 10 TO 1

Sphere Volume(mL)	10:1	R^2	Equation No.
2	y = -3.14ln(x) + 14.10	0.99	(24)
4	y = -5.54ln(x) + 24.86	0.99	(25)
8	y = -9.35ln(x) + 43.72	0.99	(26)
16	y = -14.4ln(x) + 69.00	0.99	(27)

TABLE (6): SET OF FUNCTIONS RELATING THRESHOLD AND SPHERE VOLUME AT CONTRAST RATIO 14 TO 1

Sphere Volume(mL)	14:1	R^2	Equation No.
2	y = -2.93ln(x) + 13.21	0.98	(28)
4	y = -5.74ln(x) + 24.88	0.85	(29)
8	y = -8.10ln(x) + 38.15	0.99	(30)
16	y = -13.8ln(x) + 68.20	0.99	(31)

TABLE (7): NORMALIZED ERRORS BETWEEN MEASURED AND ESTIMATED THRESHOLDS

		Volume mL	Measured threshold	Estimated threshold	Difference
Lesion /Background	3:1	2	59	67	13
		4	59	63	6.7
		8	57	59	3.5
		16	49	55	12.2
	10:1	2	47	50	6.3
		4	45	46	2.2
		8	45	42	6.6
		16	40	38	5
	14:1	2	45	45	0
		4	39	41	5
		8	38	37	2
		16	37	33	10

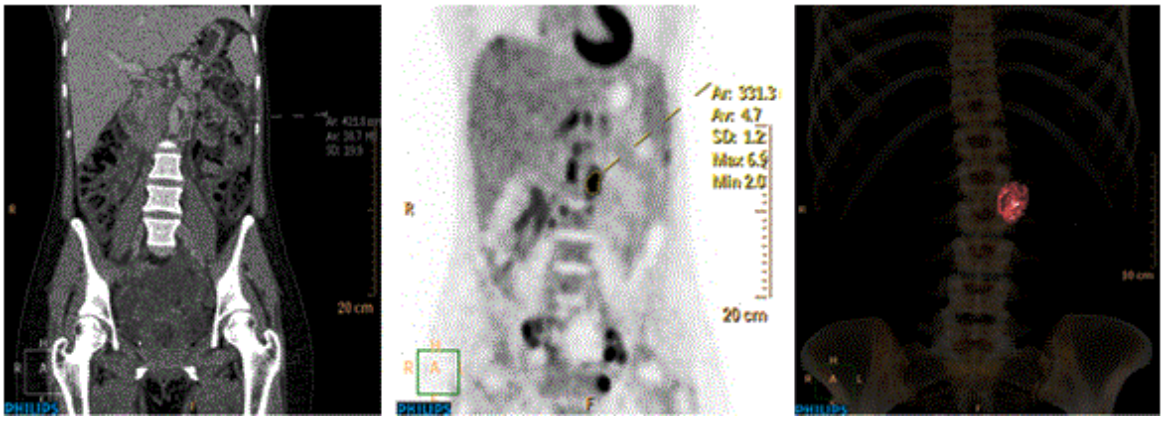

Fig. (4): An example of lesion deleniation (a) CT image (b) PET image (c) Extracted lesion volume using segmentation and its location

TABLE (8): DIFFERENT LESION VOLUMES MEASURED IN PET USING ESTIMATED THRESHOLD COMPARED TO THEIR VOLUMES MEASURED IN CT USING TISSUE SEGMENTATION TOOL AND THE ERROR

Case Number	SUVmax	SUVmean (background)	Ratio	Estimated threshold(% of SUVmax	CT volume(cm3)	PET Volume(cm3)	ERROR
1	4.2	2	2.1	71	2.6	2.7	3.8
2	5.9	1.5	3.93	58	5.3	4.7	11.3
3	6.3	1.8	3.5	58	7.5	7.4	1.3
4	5.1	1	501	52	8.4	7	16.6
5	8	0.5	16	36	7	6.3	10
6	6.9	1.9	6.63	45	13.4	12.3	8.2
7	17	1.6	10.62	33	32.2	38	18
8	4.9	1.2	4	61	2.9	2.41	17
9	7.8	1	7.8	51	3.2	3.8	18.75
10	13	1.3	10	46	4.5	4.3	4.4
11	5.8	1.2	4	47	35	38.8	10
12	12	0.7	17.14	45	45	49	8.8
13	7.5	0.7	10.7	38	14.5	13.6	6.2
14	7.4	0.6	12.3	34	18.9	22.8	20.6
15	11	0.8	13.75	42	4.4	4.2	4.5
16	7.7	1.8	4.3	49	22	25.5	15
17	12	1.7	7.1	40	29.4	30.3	3
18	16.6	1	16.6	18	143	140	2.3
19	12.4	0.8	15.5	29	29	24.8	14

The most appropriate threshold for every lesion volume is calculated from its relative trend line equation (equations 20 to 31 as illustrated in the above Tables) and the estimated values using equation (18) are given in Table(9)then measuring the error between the estimated and measured value to get the NMSE which is 6.2

Clinical application

Nineteen routine cases were selected, the size of the tumor in the CT images was measured using tissue segmentation tool. Then, the PET images were selected to measure the lesion SUV max and background SUV mean and put the value of lesion/background in the constructed equation form to get the threshold and finally determine the lesion volume to compare it with that result from CT as shown in Fig. (4).

Comparing the lesion volume in PET calculated through threshold estimation to that in CT using the tissue segmentation tool the NMSE=10.35

Discussions

The main objective of this study is to find a general equation through which we can automatically delineate lesions in PET/CT studies.

In the phantom study, the volume delineation accuracy of the relative threshold method with the SUV max was validated. In the clinical study, the impact of the suggested method was verified using the clinical FDG-PET/CT images of 19 patients randomly chosen from routine works and the lesion volumes in PET were compared to those obtained from CT segmentation.

Lesion volume definition using PET images is currently used in multiple applications. For instance, delineated lesion volume is used for the measurement of total lesion glycolysis and the delineation of gross tumor volume for radiation treatment planning [16,17].

Several volume delineation studies have been devised to improve the delineation accuracy [18, 19, and 20].

When measuring lesion volume using a relative threshold of SUV, the lesion delineation is affected, to a large extent, by the definition of the threshold. Therefore, many previous studies have focused on finding the optimal threshold to make these volume calculations [20, 21].

The optimal reported fixed threshold value that has been reported was 40% [18,22].

However, the fixed threshold value method has a limitation. It is difficult to assess tumor volume, SUV value, uniformity of SUV within the tumor .Hence, individual threshold settings for the tumor and reconstruction conditions are required to achieve accurate tumor volume measurements [18,19,21,23,24]. The current study suggests a logarithmic equation that relate the threshold value to the contrast ratio which means that the threshold value will depend on the SUV level and its background.

The proposed method in the current work on the phantom study at different contrast ratios provides a reliable tool to estimate the lesion threshold to determine the lesion volume accurately. The accuracy of this method increases with the increase of the size of the tumor. There is a need for more investigations for lesions sizes smaller than $2cm^3$ and those which are not clearly separated from any tumor in around.

The attempt made here was to optimize the threshold values that accurately segment a given PET lesion when the volume is measured with CT. A number of measurements were taken to ensure an adequate coverage of the impact of PVE on lesion size at relatively wide range of lesion to background ratio (i.e contrast ratio). Then, validation studies were conducted on different contrast ratios to verify that the generated formula (Eq.18) of the volume segmentation threshold is valid. The error associated with using an adapted threshold value was well below 10% (i.e. NMSE=6.2) when the algorithm was used in comparison to CT lesion volume. However, the error in 19 clinical lesions was about 10%.

Limitation

The method under study was valid with some limitations which need further research, these limitations are:

1- There should be a clear gap between the lesion and any nearby tumor.

2- The lesion volume should be $\geq 2cm^3$

Conclusions

This study reveals that a logarithmic 3D equation can be used to identify nearly accurate the optimal threshold value with variable contrast ratio and lesion volume in PET studies using 18F Fluorodeoxyglucose. The defined volume fluctuated in accordance with the SUV max level

and the lesion background. Thus, the equation containing lesion/background and lesion volume as variables is important to get the optimum threshold for lesion delineation. Using this method can reduce the effect of inter observer variation when measuring some quantifications such as total lesion glycolsis (TLG) and growth tumor volume (GTV).

References

1. Fletcher JW, Djulbegovic B, Soares HP, Siegel BA, Lowe VJ, Lyman GH, Coleman RE, Wahl R, Paschold JC, Avril N, Einhorn LH, Suh WW, Samson D, Delbeke D, Gorman M, Shields AF. Recommendations on the use of ^{18}F-FDG PET in oncology. J Nucl Med. 2008;49:480–508. doi: 10.2967/jnumed.107.047787
2. Van de Wiele C, Kruse V, Smeets P, Sathekge M, Maes A. Predictive and prognostic value of metabolic tumour volume and total lesion glycolysis in solid tumours. Eur J Nucl Med MolImag. 2013;40:290–301. doi: 10.1007/s00259-012-2280-z.
3. Van Baardwijk A, Baumert BG, Bosmans G, vanKroonenburgh M, Stroobants S, Gregoire V, Lambin P, De Ruysscher D. The current status of FDG-PET in tumour volume definition in radiotherapy treatment planning. Cancer Treat Rev. 2006;32:245–260. doi: 10.1016/j.ctrv.2006.02.002.
4. Wahl RL, Jacene H, Kasamon Y, Lodge MA. From RECIST to PERCIST: evolving considerations for PET response criteria in solid tumors. J Nucl Med. 2009;50 (Suppl 1):122S–150S. doi: 10.2967/jnumed.108.057307.
5. Van Baardwijk A, Bosmans G, Boersma L, Buijsen J, Wanders S, Hochstenbag M, van Suylen R-J, Dekker A, Dehing-Oberije C, Houben R, Bentzen SM, van Kroonenburgh M, Lambin P, De Ruysscher D. PET-CT-based auto-contouring in non-small-cell lung cancer correlates with pathology and reduces interobserver variability in the delineation of the primary tumor and involved nodal volumes. Int J RadiatOncolBiol Phys. 2007;68:771–778. doi: 10.1016/j.ijrobp.2006.12.067.
6. Petit S, Van EW, Oberije C, Vegt E, Dingemans A, Lambin P, Dekker A, De RD. 18F-Fluorodeoxyglucose uptake patterns in the lung before radiotherapy identify areas that are more susceptible to radiation-induced lung toxicity in non-small cell lung cancer patients. Int J RadiatOncolBiol Phys. 2011;81:698–705. doi: 10.1016/j.ijrobp.2010.06.016.
7. Cheson BD, Pfistner B, Juweid ME, Gascoyne RD, Specht L, Horning SJ, Coiffier B, Fisher RI, Hagenbeek A, Zucca E, Rosen ST, Stroobants S, Lister TA, Hoppe RT, Dreyling M, Tobinai K, Vose JM, Connors JM, Federico M, Diehl V. Revised response criteria for malignant lymphoma. J ClinOncol. 2007;25:579–586. doi: 10.1200/JCO.2006.09.2403.
8. MacManus M, Nestle U, Rosenzweig KE, Carrio I, Messa C, Belohlavek O, Danna M, Inoue T, Deniaud-Alexandre E, Schipani S, Watanabe N, Dondi M, Jeremic B. Use of PET and PET/CT for radiation therapy planning: IAEA expert report 2006-2007. RadiotherOncol. 2009;91:85–94. doi: 10.1016/j.radonc.2008.11.008.
9. Boellaard R, Krak NC, Hoekstra OS, Lammertsma AA. Effects of noise, image resolution, and ROI definition on the accuracy of standard uptake values: a simulation study. J Nucl Med. 2004;45:1519–1527.
10. Schaefer A, Kremp S, Hellwig D, Rübe C, Kirsch C-M, Nestle U. A contrast-oriented algorithm for FDG-PET-based delineation of tumour volumes for the radiotherapy of lung cancer: derivation from phantom measurements and validation in patient data. Eur J Nucl Med MolImag. 2008;35:1989–1999. doi: 10.1007/s00259-008-0875-1.
11. Geets X, Lee JA, Bol A, Lonneux M, Grégoire V. A gradient-based method for segmenting FDG-PET images: methodology and validation. Eur J Nucl Med MolImag. 2007;34:1427–1438. doi: 10.1007/s00259-006-0363-4.
12. Van Dalen JA, Hoffmann AL, Dicken V, Vogel WV, Wiering B, Ruers TJ, Karssemeijer N, Oyen WJG. A novel iterative method for lesion delineation and volumetric quantification with FDG PET. Nucl Med Commun. 2007;28:485–493. doi: 10.1097/MNM.0b013e328155d154.
13. Hatt M, Cheze le Rest C, Turzo A, Roux C, Visvikis D. A fuzzy locally adaptive Bayesian segmentation approach for volume determination in PET. IEEE Trans Med Imag. 2009;28:881–893. doi: 10.1109/TMI.2008.2012036.
14. Cheebsumon P, Boellaard R, de Ruysscher D, van Elmpt W, van Baardwijk A, Yaqub M, Hoekstra OS, Comans EF, Lammertsma AA, van Velden FH. Assessment of tumour size in PET/CT lung cancer studies: PET- and CT-based methods compared to pathology. EJNMMI Res. 2012;2:56. doi: 10.1186/2191-219X-2-56.

15. Shepherd T, Teräs M, Beichel RR, Boellaard R, Bruynooghe M, Dicken V, Gooding MJ, Julyan PJ, Lee JA, Lefevre S, Mix M, Naranjo V, Wu X, Zaidi H, Zeng Z, Minn H. Comparative study with new accuracy metrics for target volume contouring in PET image guided radiation therapy. IEEE Trans Med Imag. 2012;31:2006–2023. doi: 10.1109/TMI.2012.2202322.
16. Larson SM, Erdi Y, Akhurst T, Mazumdar M, Macapinlac HA, Finn RD, et al. Tumor treatment response based on visual and quantitative changes in global tumor glycolysis using PET-FDG imaging. The visual response score and the change in total lesion glycolysis. Clin Positron Imaging. 1999;2(3):159–71.
17. Kitajima K, Suenaga Y, Ueno Y, Maeda T, Ebina Y, Yamada H, et al. Preoperative risk stratification using metabolic parameters of 18F-FDG PET/CT in patients with endometrial cancer. Eur J Nucl Med Mol Imaging. 2015;42(8):1268–75.
18. Nestle U, Kremp S, Schaefer-Schuler A, Sebastian-Welsch C, Hellwig D, Rübe C, et al. Comparison of different methods for delineation of 18F-FDG PET–positive tissue for target volume definition in radiotherapy of patients with non-small cell lung cancer. J Nucl Med. 2005;46(8):1342–8.
25. single standardized uptake value threshold approach appropriate? J Nucl Med. 2006;47(11):1808–12.
19. Firouzian A, Kelly MD, Declerck JM. Insight on automated lesion delineation methods for PET data. EJNMMI Res. 2014;4:69.
20. Kao CH, Hsieh TC, Yu CY, Yen KY, Yang SN, et al. 18F-FDG PET/CT-based gross tumor volume definition for radiotherapy in head and neck cancer: a correlation study between suitable uptake value threshold and tumor parameters. Radiat Oncol. 2010;5:76.
21. Jentzen W, Freudenberg L, Eising EG, Heinze M, Brandau W, Bockisch A. Segmentation of PET volumes by iterative image thresholding. J Nucl Med. 2007;48(1):108–14.
22. Brianzoni E, Rossi G, Ancidei S, Berbellini A, Capoccetti F, Cidda C, et al. Radiotherapy planning: PET/CT scanner performances in the definition of gross tumour volume and clinical target volume. Eur J Nucl Med Mol Imaging. 2005;32(12):1392–9.
23. Hatt M, Cheze-le Rest C, van Baardwijk A, Lambin P, Pradier O, Visvikis D. Impact of tumor size and tracer uptake heterogeneity in 18F-FDG PET and CT non-small cell lung cancer tumor delineation. J Nucl Med. 2011;52(11):1690–7.
24. Biehl KJ, Kong FM, Dehdashti F, Jin JY, Mutic S, El Naqa I, et al. 18F-FDG PET definition of gross tumor volume for radiotherapy of non-small cell lung cancer: is a